(A New Proposal to Jefferson Lab PAC-26)
A Measurement of the Flavor Asymmetry through Charged Meson Production in Semi-Inclusive Deep-Inelastic Scattering

X. Zheng
Argonne National Laboratory, Argonne, Illinois.

D. Dutta, H. Gao, K. Kramer, X. Qian, W. Xu, Q. Ye, X. Zong
Duke University, Durham, North Carolina.

P. Markowitz
Florida International University, Miami, Florida.

H. Hiejima, A. Nathan, J.-C. Peng (Co-Spokesperson), L. Y. Zhu (Co-Spokesperson) [a]
University of Illinois, Urbana-Champaign, Illinois.

J.-P. Chen (Co-Spokesperson), E. Chudakov, A. Deur, J. Gomez, D.W. Higinbotham, O. Hansen, C. W. de Jager, M. Jones, J. LeRose, W. Melnitchouk, R. Michaels, S. Nanda, B. Reitz, A. Saha, B. Wojtsekhowski
Jefferson Lab, Newport News, Virginia.

W. Korsch
University of Kentucky, Lexington, Kentucky.

Simon Širca
University of Ljubljana, Slovenia.

W. Bertozzi, O. Gayou, S. Gilad
Massachusetts Institute of Technology, Cambridge, Massachusetts.

J. Calarco and W. Hersman
University of New Hampshire, Durham, New Hampshire.

L. Gan
University of North Carolina, Wilmington, North Carolina.

P. Ulmer
Old Dominion University, Norfolk, Virginia.

S. Frullani, F. Garibaldi, M. Iodice, G. Urciuoli
Instituto Nazionale de Fiscica Nucleare, Sezione Sanita , Roma, Italy

F. Benmokhtar, R. Gilman, C. Glashausser, X. Jiang (Co-Spokesperson) , G. Kumbartzki, K. McCormick, R. Ransome
Rutgers University, Piscataway, New Jersey.

T. Ruan, Y. Ye, Z. Yin, J. Shen, Y. Jiang

[a] Contact person. Email: lyzhu@jlab.org

University of Science and Technology of China, Hefei, China.

S. Zhou, J. Yuan
China Institute of Atomic Energy, Beijing, China.

F. Butaru, Seonho Choi, Z.-E. Meziani, K. Slifer, P. Solvignon, N. Ploquin, H. Yao
Temple University, Philadelphia, Pennsylvania.

G. Cates, R. Lindgren, N. Liyanage, V. Nelyubin, B. Norum, K. Wang
University of Virginia, Charlottesville, Virginia.

T. Averett, T. Holmstrom, V. Sulkosky
College of William and Mary, Williamsburg, Virginia.

and the Hall A Collaboration.

Abstract

We propose to measure the semi-inclusive $(e, e'\pi^{\pm})$ and $(e, e'K^{\pm})$ reactions on both hydrogen and deuterium targets in the kinematic range of $0.1 < x < 0.4$, $1.1 < Q^2 < 2.7$ GeV^2, $2.5 < W < 3.1$ GeV and $0.3 < z < 0.7$ in JLab Hall A with a 6 GeV electron beam.

Preliminary data from E00-108[1] have shown[2] that a generalized form of factorization between the virtual photon-quark hard scattering process and quark hadronization can describe the data in optimized JLab kinematic regions.

With the factorization, the charge pion yield ratio can be related to $(d + \bar{d})/(u + \bar{u})$ and $(d - \bar{d})/(u - \bar{u})$. The proposed measurement will determine the above ratios to better than 0.015 (0.02) and 0.03 (0.01) statistical (systematic) precisions respectively, to provide strong constraints on the quark flavor asymmetries. The precision of measured $(\bar{d} - \bar{u})/(u - d)$ will improve by more than a factor of 5 over the HERMES measurement, the best available world measurement from lepton scattering, and will also extend to the higher x region. The extracted $\bar{d}/\bar{u}$ results will have a comparable precision to the Fermilab E866 data, providing a check, using an independent physics process, of the surprising drop of this ratio with increasing x at $x > 0.15$.

The measurement will also examine the flavor dependence of the fragmentation functions. In particular it will provide the first precision data on kaon production in SIDIS. The ratio of the fragmentation function for d to the kaon to that for u to the kaon (D_d^K/D_u^K) is related to the light sea quark asymmetry in the kaon. The proposed measurement will improve our knowledge on this ratio significantly.

1 Introduction

Inclusive Deep Inelastic Scattering (DIS) has been the major experimental tool to measure the unpolarized and polarized nucleon structure functions. In recent years, the semi-inclusive DIS (SIDIS), where a hadron is detected in coincidence with the scattered electron, was shown to provide additional information not accessible with inclusive DIS. In particular, the HERMES collaboration has recently studied the flavor decompositions of unpolarized and polarized parton distributions using SIDIS, and results on the $\bar{d} - \bar{u}$, Δu, Δd, $\Delta\bar{u}, \Delta\bar{d}$, and $\Delta s + \Delta\bar{s}$ have been reported [3]. Another important feature of SIDIS is that several novel parton distribution and fragmentation functions, such as transversity and the Collins function[4], could also be accessed.

Despite the unique physics potential offered by the SIDIS, our current understanding of the mechanisms of SIDIS is still rather limited. It is not evident that QCD factorization is applicable in SIDIS. It is also not clear over what kinematic domain SIDIS can be interpreted in the pQCD framework. Nevertheless, notable recent progress has been made. First, SIDIS data from HERMES[3] and from the recent JLab Hall-C (E00-108)[2] experiment showed that the data are consistent with factorization. A very recent theoretical work also showed that QCD factorization is valid for SIDIS with hadrons emitted in the current fragmentation region with low transverse momentum[5]. Additional precise experimental data are clearly needed to further advance our understanding of the SIDIS.

We propose to carry out a high-statistics semi-inclusive electron scattering experiment at Hall-A. There are two major goals of this proposed experiment. First, a new measurement of the sea-quark asymmetry, $\bar{d}-\bar{u}$, will be obtained over the range $0.1 < x < 0.4$ with a 5-fold improvement in statistical accuracy over the previous HERMES measurement. Second, a first test of the $\bar{u}/\bar{d}$ flavor asymmetry of the kaon fragmentation functions will be performed using the kaon SIDIS data. In addition, the validity of factorization in SIDIS will be tested with charged pion and kaon SIDIS for the kinematic condition of this experiment. In the rest of this Section, we describe the physics motivation and the proposed approach.

1.1 Flavor asymmetry of the nucleon sea

The earliest parton models assumed that the proton sea was flavor symmetric, even though the valence quark distributions are clearly flavor asymmetric. The flavor symmetry assumption was not based on any known physics, and it remained to be tested.

The first indication of the inequality of $\bar{u}(x)$ and $\bar{d}(x)$ came from measurements of the Gottfried integral[6] which is defined as:

$$I_G = \int_0^1 \left[F_2^p(x,Q^2) - F_2^n(x,Q^2)\right] \frac{dx}{x} \tag{1}$$

where F_2^p and F_2^n are the proton and neutron structure functions measured in deep inelastic scattering experiments. In terms of the valence and sea quark distributions of the proton, under the assumption of isospin symmetry, I_G can be expressed as:

$$I_G = \frac{1}{3}\int_0^1 \left[u_v(x,Q^2) - d_v(x,Q^2)\right] dx + \frac{2}{3}\int_0^1 \left[\bar{u}(x,Q^2) - \bar{d}(x,Q^2)\right] dx \tag{2}$$

A flavor-symmetric nucleon sea ($\bar{u}(x) = \bar{d}(x)$) would lead to $\mathrm{I}_G = 1/3$, the Gottfried sum rule[6]. Measurements by the New Muon Collaboration (NMC)[7] determined that $\int_{0.004}^{0.8} \left[F_2^p(x) - F_2^n(x)\right]/x \; dx = 0.221 \pm 0.021$ at $Q^2 = 4$ GeV^2. Extrapolating to $x = 0$ through the unmeasured small-x region, they projected that $\mathrm{I}_G = 0.235 \pm 0.026$, significantly below 1/3. Specifically, the NMC result implies that $\int_0^1 \left[\bar{d}(x) - \bar{u}(x)\right] dx = 0.148 \pm 0.039$. While no known symmetry requires $\bar{u}$ to equal $\bar{d}$, a large $\bar{d}/\bar{u}$ asymmetry was not anticipated. Many ideas such as Pauli blocking and pion clouds have been proposed to explain such a flavor asymmetry in the sea[8]. Two methods have been suggested to measure its x-dependence: the Drell-Yan process[9] and the semi-inclusive deep inelastic scattering[10].

Recently, Fermilab experiment E866 reported measurements of the yield ratio of Drell-Yan muon pairs from an 800 GeV/c proton beam incident on hydrogen and deuterium[11]. The data suggested a significantly asymmetric light-quark sea distribution over an appreciable range in x; the asymmetry peaked around $x = 0.13$. The ratio of the Drell-Yan cross section

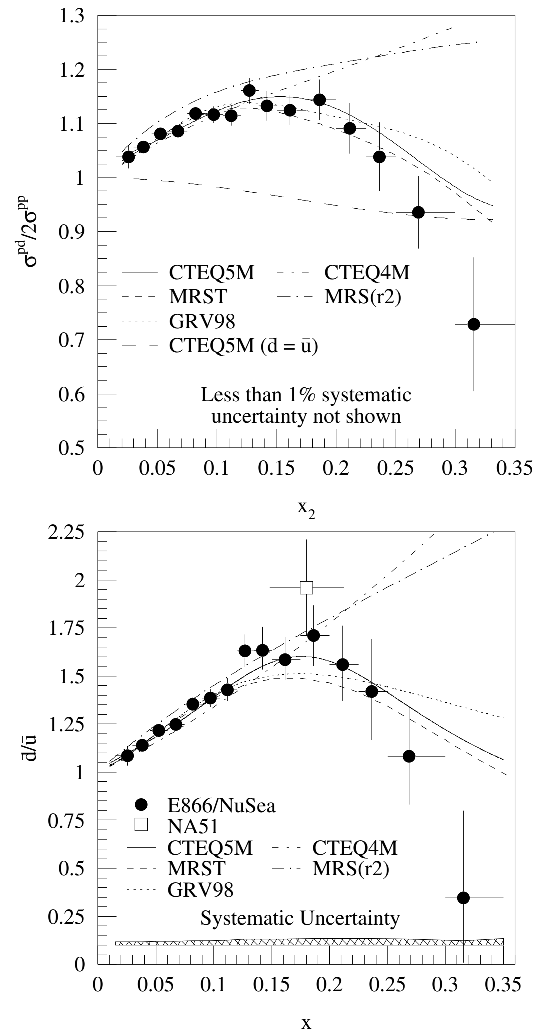

Figure 1: Fermilab E866 results. The upper plot shows the ratio of $\sigma^{pd}/2\sigma^{pp}$ of Drell-Yan cross sections vs the target quark momentum fraction x. The lower dashed line shows the CTEQ5M curve while taking $\bar{d} - \bar{u} = 0$. The lower plot shows the ratio of $\bar{d}/\bar{u}$ as a function of x. The result from CERN experiment NA51 is shown as an open box.

per nucleon for p+d to that of p+p is shown in Fig. 1. Assuming isospin symmetry, the Drell-Yan ratio can be expressed as:

$$\frac{\sigma^{pd}}{2\sigma^{pp}} \approx \frac{1}{2}\left(1 + \frac{\bar{d}_2}{\bar{u}_2}\right), \tag{3}$$

where the subscript 2 indicates the beam quark (1 would be for target quark). Assuming $\bar{d} + \bar{u}$ distributions are accurate in global fits of quark distributions, such as CTEQ5M [12] (and MRST [13]), E866 extracted $\bar{d}/\bar{u}$ from the measured Drell-Yan ratio, as shown in Fig. 1.

Many theoretical models, including meson cloud model, chiral-quark model, Pauli-blocking model, instanton model, chiral-quark soliton model, and statistical model, have been proposed to explain the $\bar{d}/\bar{u}$ asymmetry. For recent reviews, see [14,15]. These models can describe the $\bar{d} - \bar{u}$ data very well. However, they all have difficulties explaining the $\bar{d}/\bar{u}$ data at large x ($x > 0.2$). Since the perturbative process gives a symmetric sea for u and d (i.e., $\bar{d} = \bar{u}$) while a non-perturbative process is needed to generate an asymmetric sea, the relative importance of these two components is directly reflected in the $\bar{d}/\bar{u}$ ratios. Unfortunately, due to limited statistics, the uncertainty of the E866 data is larger in this region. In the region of $0.156 < x < 0.312$, E866 $\bar{d}/\bar{u}$ results also rely on the knowledge of $\bar{d} + \bar{u}$ from earlier experimental data. Therefore, independent confirmation of sea quark distributions from different reaction channels could help to clarify the issue. The semi-inclusive $(e, e'\pi^{\pm})$ reaction is one natural choice because of the advantage in flavor tagging.

1.2 Semi-inclusive pion production in electron scattering

Semi-inclusive reactions in electron scattering can be used as a tool to study the density distributions of valence quarks as well as sea quarks. Specifically, pion electro-production on hydrogen and deuterium offers a unique probe of light quark and anti-quark distributions. At high enough energy transfer, the Independent Factorization between the virtual photon-quark hard scattering process and the hadronization of the struck quark means the parton distribution functions are z-independent and the fragmentation functions are x-independent. This leads to:

$$Y^{\pi^{\pm}}(x,z) \propto \sum_i e_i^2 \left[q_i(x) D_{q_i}^{\pi^{\pm}}(z) + \bar{q}_i(x) D_{\bar{q}_i}^{\pi^{\pm}}(z)\right], \tag{4}$$

where $Y^{\pi^{\pm}}(x,z)$ is the π^+ (π^-) yield in deep-inelastic scattering, $z = E^{\pi}/\nu$ is the fraction of the virtual photon energy carried by the pion, e_i is the quark charge and the subscript i refers to the target quark flavor. The fragmentation functions $D_{q_i}^{\pi^{\pm}}(z)$ represent the probability that a quark of flavor i fragments into a charged pion. Assuming isospin symmetry and charge conjugation invariance, the number of light quark fragmentation functions is reduced to two types: the favored (D^+) and the unfavored (D^-) fragmentation functions:

$$D^+ \equiv D_u^{\pi^+} = D_d^{\pi^-} = D_{\bar{u}}^{\pi^-} = D_{\bar{d}}^{\pi^+}, \tag{5}$$

$$D^- \equiv D_u^{\pi^-} = D_d^{\pi^+} = D_{\bar{u}}^{\pi^+} = D_{\bar{d}}^{\pi^-}. \tag{6}$$

The HERMES collaboration recently published data [3] on the ratio of $(\bar{d} - \bar{u})/(u - d)$ in the kinematic range of $0.02 < x < 0.3$ and $1 < Q^2 < 10$ GeV^2. Through measurements of the yield ratio

$$r(x,z) = \frac{Y_p^{\pi^-}(x,z) - Y_n^{\pi^-}(x,z)}{Y_p^{\pi^+}(x,z) - Y_n^{\pi^+}(x,z)}, \tag{7}$$

the flavor asymmetry was determined as:

$$\frac{\bar{d}(x) - \bar{u}(x)}{u(x) - d(x)} = \frac{J(z)[1 - r(x,z)] - [1 + r(x,z)]}{J(z)[1 - r(x,z)] + [1 + r(x,z)]}, \tag{8}$$

in which $J(z) = \frac{3}{5}\left(\frac{1+D'(z)}{1-D'(z)}\right)$ with $D'(z) = D_u^{\pi^-}/D_u^{\pi^+}$. The HERMES extraction of $(\bar{d} - \bar{u})$ are shown in Fig. 2. To obtain $(\bar{d} - \bar{u})$, in addition to the measured ratio of $(\bar{d} - \bar{u})/(u - d)$, the values of $(u - d)$ taken from the GRV-94 leading order parameterization [16] were used. Within the large statistical uncertainties, the HERMES data agree with E866 results, even though the Q^2 of the two experiments differs by a factor of about 20.

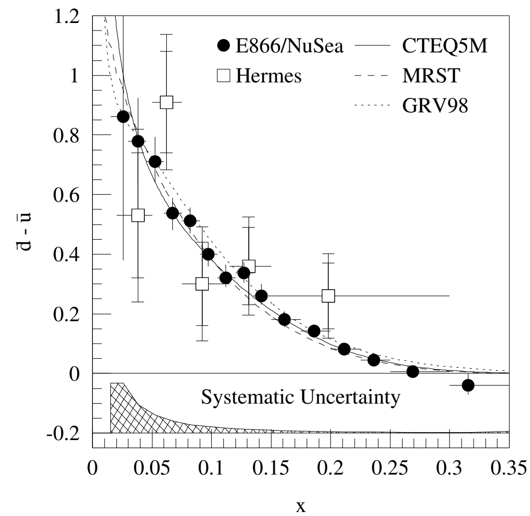

Figure 2: HERMES results of $\bar{d} - \bar{u}$ as a function of x. The open circles represent the E866 determination of $\bar{d} - \bar{u}$ at Q^2=54.0 GeV^2.

To demonstrate the evidence of factorization, HERMES also measured [3] the ratio of $(\bar{d} - \bar{u})/(u - d)$ as a function of z as shown in Fig. 3 for five x-bins. Since no indication of z dependence was observed within the experimental uncertainty (of better than 0.1), the data are consistent with the form of factorization as in Eq. 4. We note that this evidence of factorization occurred at $1.33 < Q^2 < 4.88$ GeV^2, with the requirement that the invariant mass $W > 2.0$ GeV, which is accessible at Jefferson Lab with a beam energy of 6.0 GeV.

Recently, a measurement (E00-108) [1] was performed in Hall C to study quark-hadron duality and test low energy factorization in meson electroproduction. Preliminary results [2] showed that the data are consistent with factorization in optimized JLab kinematics. Figure 4 shows one example of the preliminary E00-108 data. The E00-108 semi-inclusive π^- production cross sections are in good agreement, in the region $0.35 < z < 0.7$, with a Monte Carlo simulation assuming a fragmentation ansatz. Even at relatively low W' (down to about 1.5 GeV), the data show no evidence of significant violation of factorization.

1.3 Semi-inclusive pion production at JLab Hall-A.

In this proposal, we will measure the semi-inclusive π^+ (K^+) and π^- (K^-) yield on proton and deuteron targets with high statistical accuracy in the kinematic range of $0.1 < x < 0.4$, $1 < Q^2 < 3$ GeV^2, and $2.5 < W < 3.1$ GeV. The invariant mass of the hadron system without the detected pion will be in the range of $1.8 < W' < 2.6$ GeV. The data below $W' = 1.8$ GeV will come in at the same time, and will be used only for testing the factorization, i.e. the z-independence study. (Note: the discussion below will be focused on the pion case but most of the discussion could also apply to the kaon case. The physics focus of the kaon production will be on the flavor dependence of the fragmentation functions, to be discussed in a separate section.) Through a measurement at different z, we will test the z-independence of the yield ratios as reported by HERMES in order to demonstrate the evidence of factorization. In the case that a generalized factorization applies between the virtual photon-quark hard scattering process and the hadronization of the struck quark, a precise measurement of pion

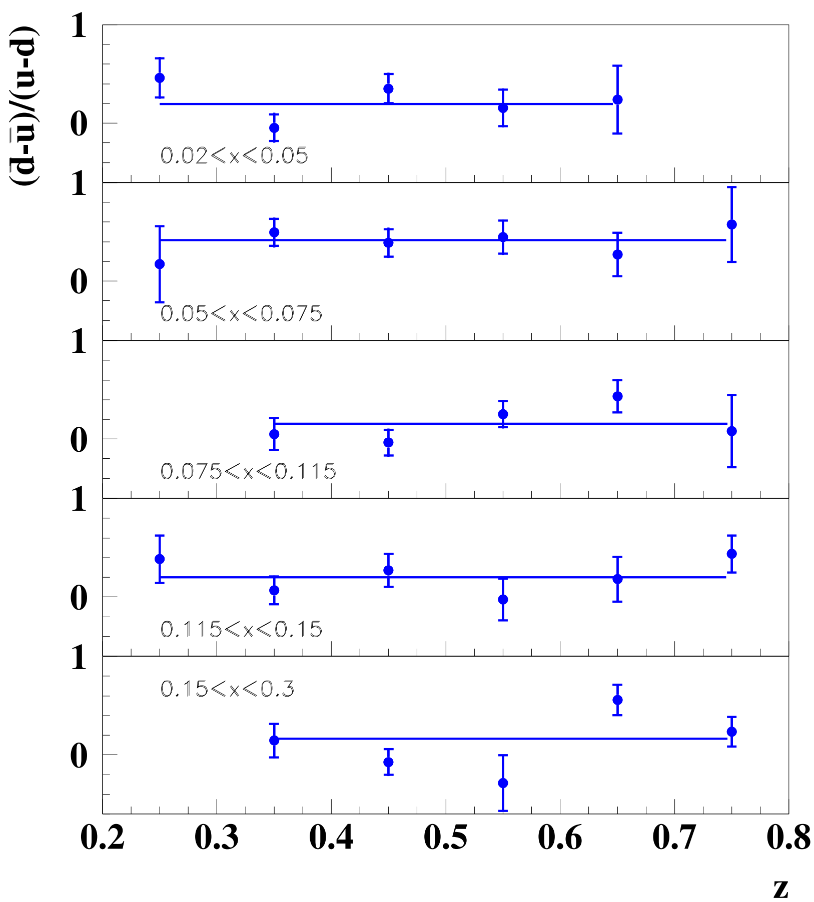

Figure 3: HERMES evidence of factorization. The distribution of $(\bar{d}-\bar{u})/(u-d)$ as a function of z in five bins of x.

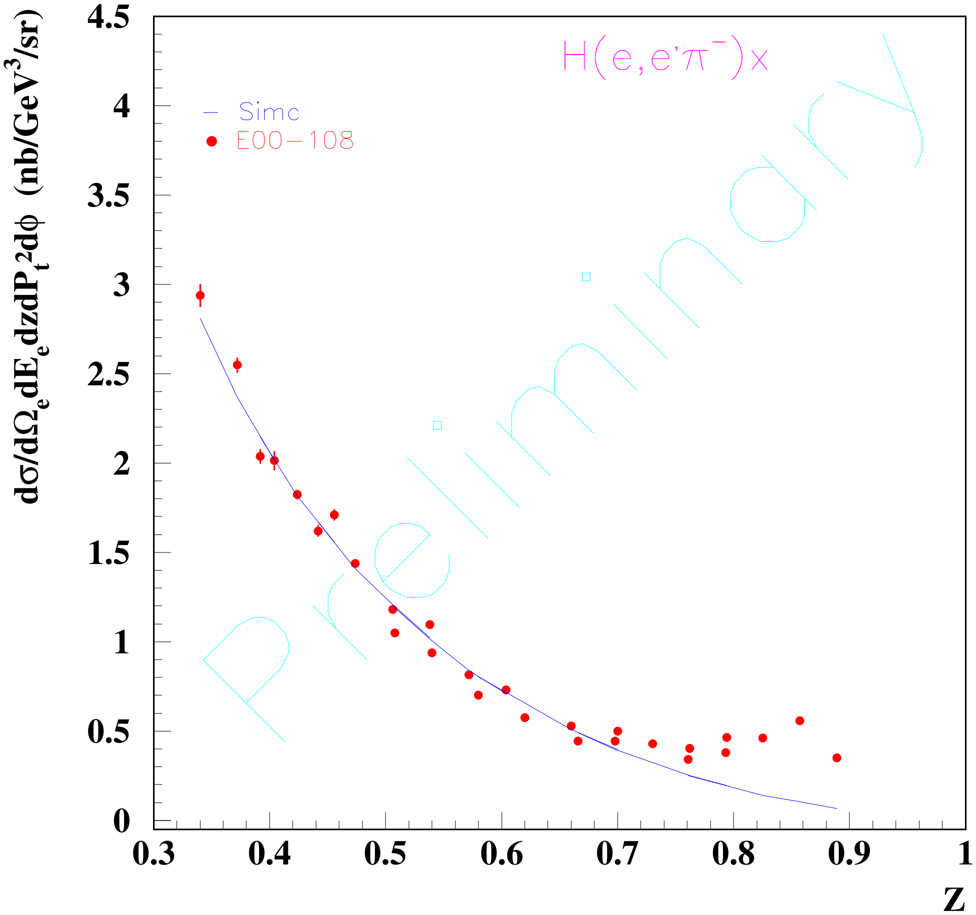

Figure 4: Preliminary E00-108 semi-inclusive π^- production cross sections (red points) at $x = 0.32$ as a function of z in comparison with a Monte Carlo simulation (solid curve) starting from a fragmentation ansatz. The scatter of the data is due to having preformed only a rudimentary bin centering.

yield ratios can be used as independent constraints in the determination of valence quark and sea quark distributions.

Assuming isospin symmetry (i.e. $u_p(x) = d_n(x)$, $d_p(x) = u_n(x)$, $\bar{u}_p(x) = \bar{d}_n(x)$, $\bar{d}_p(x) = \bar{u}_n(x)$) and neglecting heavy quark contributions, under the condition of Independent Factorization of Eq. 4, the yield of $\pi^\pm$ in deep inelastic scattering on the proton and neutron can be expressed as:

$$\begin{aligned}
Y_p^{\pi^+}(x,z) &= A\left(4u(x)D^+(z) + d(x)D^-(z) + 4\bar{u}(x)D^-(z) + \bar{d}(x)D^+(z)\right), \\
Y_p^{\pi^-}(x,z) &= A\left(4u(x)D^-(z) + d(x)D^+(z) + 4\bar{u}(x)D^+(z) + \bar{d}(x)D^-(z)\right), \\
Y_n^{\pi^+}(x,z) &= A\left(4d(x)D^+(z) + u(x)D^-(z) + 4\bar{d}(x)D^-(z) + \bar{u}(x)D^+(z)\right), \\
Y_n^{\pi^-}(x,z) &= A\left(4d(x)D^-(z) + u(x)D^+(z) + 4\bar{d}(x)D^+(z) + \bar{u}(x)D^-(z)\right).
\end{aligned} \tag{9}$$

where A is a common kinematic factor.

If four independent yields ($Y_p^{\pi^+}, Y_p^{\pi^-}, Y_n^{\pi^+}$ and $Y_n^{\pi^-}$) are measured, ratios of yields can be formed in which the fragmentation functions cancel each other:

$$t_1(x) = \frac{Y_p^{\pi^+}(x,z) + Y_p^{\pi^-}(x,z)}{Y_n^{\pi^+}(x,z) + Y_n^{\pi^-}(x,z)} = \frac{4u(x) + d(x) + 4\bar{u}(x) + \bar{d}(x)}{4d(x) + u(x) + 4\bar{d}(x) + \bar{u}(x)}, \tag{10}$$

$$t_2(x) = \frac{Y_p^{\pi^+}(x,z) - Y_p^{\pi^-}(x,z)}{Y_n^{\pi^+}(x,z) - Y_n^{\pi^-}(x,z)} = \frac{4u(x) - d(x) - 4\bar{u}(x) + \bar{d}(x)}{4d(x) - u(x) - 4\bar{d}(x) + \bar{u}(x)}. \tag{11}$$

Or simply as:

$$r_1(x) = \frac{4 - t_1(x)}{4t_1(x) - 1} = \frac{d(x) + \bar{d}(x)}{u(x) + \bar{u}(x)} = \frac{d_v(x) + 2\bar{d}(x)}{u_v(x) + 2\bar{u}(x)} \tag{12}$$

and

$$r_2(x) = \frac{4 + t_2(x)}{4t_2(x) + 1} = \frac{d(x) - \bar{d}(x)}{u(x) - \bar{u}(x)} = \frac{d_v(x)}{u_v(x)}, \tag{13}$$

in which $u_v(x) = u(x) - \bar{u}(x)$ and $d_v(x) = d(x) - \bar{d}(x)$.

In the above formalism, we've omitted the notation of Q^2 dependence of the ratios and distribution functions.

Clearly, observation of $r_1 \neq r_2$ would serve as direct evidence of a non-vanishing sea-quark distribution. Furthermore, a precise measurement of r_1 and r_2 at different x and Q^2 will provide strong and independent constraints on the parton distribution functions, especially in the high-x region where existing data lack accuracy.

We note that the Independent Factorization condition of Eq. 4 is not an absolute requirement in the cancellation of fragmentation functions in the derivation of Eqs. 12 and 13. A much more relaxed form of factorization can be tolerated. The fragmentation functions can take a more general form, for example $D = D(\nu, Q^2, z)$. As long as the fragmentation functions do not explicitly depend on the quark distributions, and as long as isospin and charge conjugation symmetry hold between different fragmentation functions, the ratios r_1 and r_2 will be independent of z and the fragmentation functions. We will refer to this relaxed form of factorization as the Generalized Factorization Condition. A clear signature of the onset of the generalized factorization will be the scaling behavior of r_1 and r_2 at different values of z. In this experiment, we propose to measure r_1 and r_2 with high precision in order to clearly demonstrate the validity of generalized factorization at each kinematic setting. We also note that exact knowledge about the fragmentation functions is not needed in

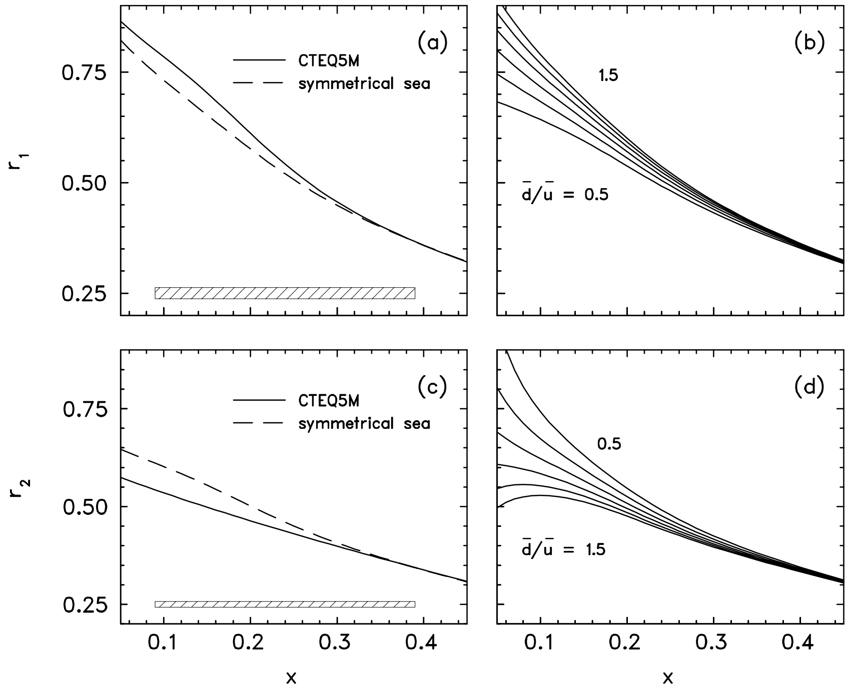

Figure 5: The quantities r_1 and r_2 at Q^2=2.23 GeV^2 from CTEQ5M predictions. The dashed lines represent the values when $\bar{d} - \bar{u} = 0$ is forced while $\bar{d} + \bar{u}$ is fixed by CTEQ5M. In plots (b) and (d) six different $\bar{d}/\bar{u}$ values uniformly spread from 0.5 to 1.5 are assumed in the CTEQ5M predictions.

this experiment because they cancel out in the yield ratios. The predicted values of r_1 and r_2 at Q^2=2.23 GeV^2 are plotted in Fig. 5 from CTEQ5M predictions. The sensitivity of r_1 and r_2 to different values of $\bar{d}/\bar{u}$ ratios is also shown, with the value of $\bar{d}+\bar{u}$ fixed by CTEQ5M.

We plan to extract the neutron yield from the deuteron and hydrogen yield difference. Nuclear binding effects and corrections due to Fermi motion are expected to be small in the region of $0.1 < x < 0.4$. [17]. Under the assumption that $Y_D^{\pi^\pm} = Y_n^{\pi^\pm} + Y_p^{\pi^\pm}$, r_1 and r_2 can be expressed as:

$$r_1 = -1 + \frac{3}{5\rho_1 - 1}, \tag{14}$$

$$r_2 = -1 + \frac{5}{3\rho_2 + 1}, \tag{15}$$

where

$$\rho_1 = \frac{Y_p^{\pi^+} + Y_p^{\pi^-}}{Y_D^{\pi^+} + Y_D^{\pi^-}}, \tag{16}$$

$$\rho_2 = \frac{Y_p^{\pi^+} - Y_p^{\pi^-}}{Y_D^{\pi^+} - Y_D^{\pi^-}} \tag{17}$$

are measured directly from experiment. The measurement uncertainties $\delta\rho_1$ and $\delta\rho_2$ propagate to r_1 and r_2 through:

$$\delta r_1 = \frac{5}{3}(1 + r_1)^2 \delta\rho_1, \tag{18}$$

$$\delta r_2 = \frac{3}{5}(1+r_2)^2 \delta\rho_2.$$

Thus, to improve the precision on r_1 and r_2 one needs to minimize $\delta\rho_1$ and $\delta\rho_2$. This implies that one should measure the yield from hydrogen and deuterium with similar relative accuracy and measure the π^+ and π^- yields with similar absolute accuracy for each target.

We will extract $(\bar{d}-\bar{u})/(u-d)$ the same way as HERMES did; see equation 8. Here, the ratio of unfavored to favored fragmentation, $D'(z)$, has to be used. The $D'(z)$ was extracted [3] from semi-inclusive charged pion production from hydrogen, deuterium and helium-3 targets, using leading order parton distribution functions [16]. Their results from different targets are consistent with each other within statistical errors. We will extract $D'(z)$ from our data and compare with the values extracted from HERMES. We can also extract $D'(z)$ from the data at the highest x where the sea contributions are small and the valence parton distributions are well determined.

1.4 Charged kaon production in SIDIS

Existing SIDIS data on charged kaon production have limited statistical accuracy. Since charged kaons can be measured simultaneously with the pions in the proposed experiment, we discuss the specific observables and physics which can be addressed with the detection of charged kaons.

Factorization and valence quark ratio

By convention, the kaon fragmentation functions are grouped into three different types, namely,

$$D_K^+ \equiv D_u^{K^+} = D_{\bar{u}}^{K^-} = D_{\bar{s}}^{K^+} = D_s^{K^-}, \tag{19}$$

$$D_K^- \equiv D_{\bar{u}}^{K^+} = D_u^{K^-} = D_s^{K^+} = D_{\bar{s}}^{K^-}. \tag{20}$$

$$D_K^d \equiv D_d^{K^+} = D_{\bar{d}}^{K^+} = D_d^{K^-} = D_{\bar{d}}^{K^-}. \tag{21}$$

Note that D_K^+ is the favored fragmentation function, while the D_K^- and D_K^d are the unfavored fragmentation functions. Under the assumption of factorization, the yields for charged kaon production in SIDIS on proton and neutron can be written as (x and z dependences are omitted for clarity):

$$\begin{aligned}
Y_p^{K^+} &= A\left(4u\ D_K^+ + d\ D_K^d + 4\bar{u}\ D_K^- + \bar{d}\ D_K^d + s\ D_K^- + \bar{s}\ D_K^+\right), \qquad (22)\\
Y_p^{K^-} &= A\left(4u\ D_K^- + d\ D_K^d + 4\bar{u}\ D_K^+ + \bar{d}\ D_K^d + s\ D_K^+ + \bar{s}\ D_K^-\right),\\
Y_n^{K^+} &= A\left(4d\ D_K^+ + u\ D_K^d + 4\bar{d}\ D_K^- + \bar{u}\ D_K^d + s\ D_K^- + \bar{s}\ D_K^+\right),\\
Y_n^{K^-} &= A\left(4d\ D_K^- + u\ D_K^d + 4\bar{d}\ D_K^+ + \bar{u}\ D_K^d + s\ D_K^+ + \bar{s}\ D_K^-\right),
\end{aligned}$$

where A is a common kinematic factor. From the above equation, the following relation is readily obtained:

$$t_2^K(x) = \frac{Y_p^{K^+}(x,z) - Y_p^{K^-}(x,z)}{Y_n^{K^+}(x,z) - Y_n^{K^-}(x,z)} = \frac{u(x)-\bar{u}(x)}{d(x)-\bar{d}(x)} = \frac{u_V(x)}{d_V(x)}. \tag{23}$$

Note that this relation is different from the corresponding relation for pions (see Eq. (11)). The contribution from strange quarks does not affect the validity of this relation. An independent check of the $u_V(x)/d_V(x)$ ratio can therefore be obtained from the charged kaon SIDIS data. These data also allow a direct test of factorization for kaon production.

Flavor asymmetry in the kaon fragmentation functions

The measurement of the $\bar{d}/\bar{u}$ asymmetry in the proton has clearly shown the presence of the flavor asymmetry for sea-quark distributions in the nucleons. It is natural to extend a search for such asymmetry to other hadronic systems. Alberg *et al.* [18] have considered the sea-quark distributions in hyperons, in particular, Σ^+. Their meson cloud model implies a $\bar{d}/\bar{u}$ asymmetry in the Σ^+ even larger than that of the proton. However, the opposite effect is expected from SU(3) symmetry. A Drell-Yan experiment using a Σ^+ hyperon beam has been considered for such study. Unfortunately, such an experiment appears to be extremely challenging due to the large pion, kaon, and proton components in the Σ^+ beam.

Another interesting area of investigation is in the meson sector. Do mesons have asymmetric light-quark sea distributions? Let us consider the case for the pions first. A π^+ contains u and $\bar{d}$ valence quarks. A flavor asymmetry in the pion sea would show up as $u_{sea} \neq d_{sea}$, which is equivalent to $\bar{u}_{sea} \neq d_{sea}$. This relation is equivalent to $\bar{u} \neq d$, since there are no valence $\bar{u}$ or d quarks in the π^+, However, the charge-conjugation symmetry and isospin symmetry dictate that $\bar{u} = d$ in the π^+. Therefore, the sea quark distributions in charged pions are u/d symmetric. This is readily understood in the Pauli-blocking picture. The presence of the u and $\bar{d}$ valence quarks in the π^+ would equally block the $u\bar{u}$ and the $\bar{d}d$ sea.

The situation is quite different for the kaons. Let us consider the case for the K^+, which has $u\bar{s}$ as its valence quarks. Light-quark flavor asymmetry in the kaon sea would imply $\bar{u} \neq \bar{d}$. Unlike the case for pions, there is no requirement for the equality of these two sea quark distributions based on isospin and charge-conjugation symmetry. One also anticipates such an asymmetry based on the Pauli-blocking picture. The presence of u quark in the K^+ would inhibit the $\bar{u}$ sea relative to the $\bar{d}$ sea in the K^+. Therefore, one expects $\bar{d} > \bar{u}$ in the K^+, analogous to the situation for the proton.

Can one measure the putative $\bar{u}/\bar{d}$ flavor asymmetry in the K^+? One might consider kaon-induced Drell-Yan process or electron scattering off the K-meson cloud of the nucleon, but no concrete proposals have been put forward so far.

A very promising avenue for probing the possible $\bar{u}/\bar{d}$ asymmetry in K^+ is the measurement of kaon fragmentation functions. The sea-quark flavor asymmetry would imply that $\bar{u}$ and $\bar{d}$ would have unequal probability to hadronize into a K^+, namely, $D_{\bar{u}}^{K^+} \neq D_{\bar{d}}^{K^+}$. A possible evidence for such asymmetry already exists. Kaon fragmentation functions have been extracted by Kniehl *et al.* [19] who fitted the hadron production data from e^+e^- annihilation. They obtain the following surprising result:

$$\int_{0.05}^{1} dz\ z\ D_{u,s}^{K^\pm}(z, Q_0^2) = 0.19, \quad \int_{0.05}^{1} dz\ z\ D_{d}^{K^\pm}(z, Q_0^2) = 0.25 \tag{24}$$

where

$$D_{u,s}^{K^\pm} = \frac{1}{4}(D_u^{K^+} + D_{\bar{u}}^{K^+} + D_s^{K^+} + D_{\bar{s}}^{K^+}) = \frac{1}{2}(D_u^{K^+} + D_{\bar{u}}^{K^+}) \tag{25}$$

and

$$D_d^{K^\pm} = \frac{1}{2}(D_d^{K^+} + D_{\bar{d}}^{K^+}) = D_{\bar{d}}^{K^+} \tag{26}$$

Since the favored valence quark fragmentation function, $D_u^{K^+}$, is expected to be larger than the sea-quark fragmentation function, $D_{\bar{d}}^{K^+}$, one obtains

$$\int_{0.05}^{1} dz\ z\ D_u^{K^+}(z, Q_0^2) > \int_{0.05}^{1} dz\ z\ D_{\bar{d}}^{K^+}(z, Q_0^2) = 0.25 \tag{27}$$

From Eqs. (24)-(27), we obtain

$$\int_{0.05}^{1} dz\ z\ D_{\bar{u}}^{K^+}(z, Q_0^2) < 0.065, \quad \int_{0.05}^{1} dz\ z\ D_{\bar{d}}^{K^+}(z, Q_0^2) = 0.25 \tag{28}$$

This result shows that the $\bar{d}$ quark, which is a sea quark for K^+, has a much higher probability to fragment into a K^+ than for the $\bar{u}$ sea quark. This surprising result might reflect a large $\bar{d}/\bar{u}$ flavor asymmetry in the kaon sea, resulting in a large enhancement of $\bar{d}$ over $\bar{u}$ in the kaon structure function, as well as an enhancement of the $D_{\bar{d}}^{K^+}$ fragmentation function. Clearly, additional data on kaon fragmentation function would be of great interest. We propose to measure the following quantity:

$$\frac{D_d^{K^\pm}}{D_u^{K^\pm}} \equiv \frac{2D_K^d}{D_K^+ + D_K^-} \sim 4\frac{(Y_n^{K^+} + Y_n^{K^-}) - r_1^\pi * (Y_p^{K^+} + Y_p^{K^-})}{(Y_p^{K^+} + Y_p^{K^-}) - r_1^\pi * (Y_n^{K^+} + Y_n^{K^-})}, \tag{29}$$

where r_1^π was defined earlier for the pion SIDIS and can be measured from the proposed experiment. The above relation shows that kaon SIDIS can provide an independent check of the possible flavor asymmetry of the kaon fragmentation function.

2 The Experiment

2.1 Experimental goal.

We propose to study deep inelastic semi-inclusive $(e, e'\pi^\pm)$ and $(e, e'K^\pm)$ reactions on hydrogen and deuterium at the optimized DIS conditions available to JLab at 6 GeV. We plan to measure the yield ratios r_1 and r_2 to high statistical accuracyin order to extract light quark and anti-quark distribution ratios in the nucleon. By examining the z-dependence of these ratios, we expect to test the factorization at our kinematic conditions with high precision.

The planned experiment will use the BigBite spectrometer at 30° beam-right for electron detection. The detector package will be the same as the one being assembled for the approved Hall A G_e^n (E02-013) experiment. The hadron arm will be the Hall-A HRS spectrometer with the septum magnet at 6°. The recently commissioned RICH detector, in combination with the standard detector package, will provide excellent particle identifications (PID) of pions and kaons over a wide momentum range. With the excellent PID, we will also be able to study the flavor dependence of the fragmentation functions. In particular, this experiment will provide the first precision data of Kaon electroproduction in SIDIS and will enable a study of the flavor dependence of the poorly known Kaon fragmentation functions.

2.2 Kinematics choice

The kinematic variables are defined in Fig. 6. We always use a beam energy of E=6.0 GeV. E$'$ and θ_e are the energy and angle of the scattered electron, p_π and θ_π are the momentum and lab angle of the detected pion and $z = E_\pi/\nu$. W is the invariant mass of the entire hadronic system and W' is the invariant mass of the hadronic system without the detected pion.

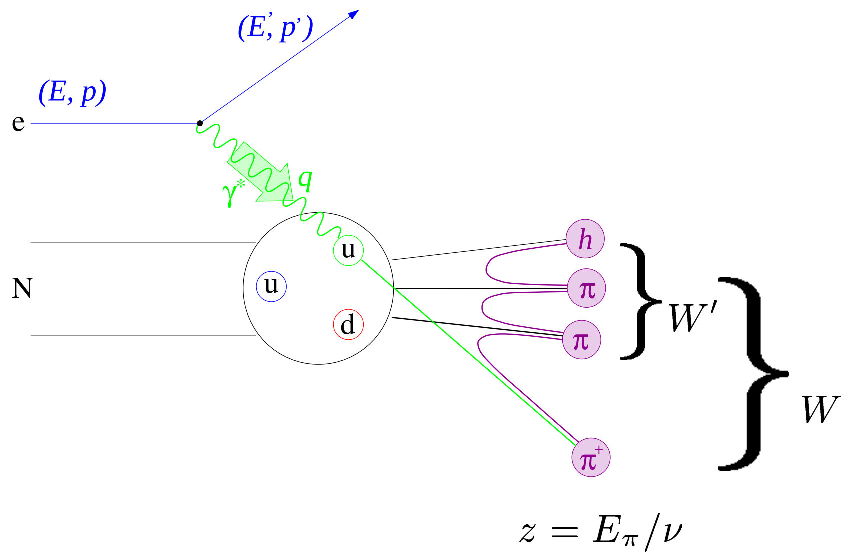

Figure 6: Diagram of (e,e'π) reaction on nucleon.

We chose to cover the region of $0.1 < x < 0.4$ and the highest possible W with 6 GeV beam in order to be as far as possible into the deep inelastic region. We also chose to detect the fragmentation products directly along the momentum transfer with 35% $\sim$ 65% of total energy transfer to favor the current fragmentation regime rather than the target fragmentation regime. The W' are also chosen to be the highest possible (1.8 GeV to 2.6 GeV) to avoid contributions from resonance structures. These choices make the direction of $\vec{q}$ very close to the beam line; thus, the use of the septum magnet is necessary. Because the design of the septum magnet moves the interaction points 80 cm upstream of the regular target location, the other HRS spectrometer cannot be used at an angle larger than 12.3°. The BigBite spectrometer will be used as our electron arm, which has an advantage of a much larger acceptance in both angle and momentum.

Within one BigBite setting, the finite solid angle acceptance ($\Delta\Omega = 36$ msr at 2.4 meter drift) and large momentum bite (at least 0.6$\sim$1.8 GeV) allow a wide kinematic region to be covered. If we take six uniform E' bins between 0.6$\sim$1.8 GeV, the corresponding coverage in the (x, W) plane and in the (x, Q^2) plane are shown in Fig. 7.

We will take four HRS momentum settings from 1.7 to 3.2 GeV/c to cover z from 0.32 to 0.70. The available phase space in the (x, W') and (x, p_t) planes for each HRS momentum setting is shown in Fig. 8. Within each setting, several bins of E' are plotted following the same color code in Fig. 7.

1

Table 1: Central kinematic values for each E'-bin. The beam energy is $E = 6.0$ GeV. Four hadron arm momentum settings will be taken. E' (GeV) and θ_e (degree) are electron arm momentum and angle. Singles electron rates for each bin are listed for the Hydrogen target case with 5 μA of beam current. The hadron arm angle is fixed at 6°, and P_π (GeV/c) is the hadron arm momentum. W (in GeV) is the invariant mass of the hadron system, W' (in GeV) is the invariant mass of the hadron system without the detected pion. The kinematic settings in parentheses are the ones with W' less than 1.8 GeV and will only be used for z-dependence (factorization) study, but not used for parton distribution extractions.

E'	θ_e	$\langle x \rangle$	W	Q^2	$\text{Rate}_{(e,e')}$ (Hz)	P_π	z	W'
0.700	30.0	0.11	3.11	1.13	655.8			
						1.70	0.32	2.61
						2.20	0.42	2.45
						2.70	0.51	2.27
						3.20	0.60	2.08
0.900	30.0	0.15	3.00	1.45	545.7			
						1.70	0.33	2.50
						2.20	0.43	2.34
						2.70	0.53	2.16
						3.20	0.63	1.97
1.100	30.0	0.19	2.88	1.77	460.7			
						1.70	0.35	2.38
						2.20	0.45	2.22
						2.70	0.55	2.04
						3.20	0.65	1.85
1.300	30.0	0.24	2.76	2.09	389.5			
						1.70	0.36	2.26
						2.20	0.47	2.10
						2.70	0.58	1.92
						(3.20	0.68	1.72)
1.500	30.0	0.29	2.63	2.41	324.0			
						1.70	0.38	2.13
						2.20	0.49	1.97
						2.70	0.60	1.79
						(3.20	0.71	1.59)
1.700	30.0	0.34	2.49	2.73	261.5			
						1.70	0.40	1.99
						2.20	0.51	1.83
						(2.70	0.63	1.65)

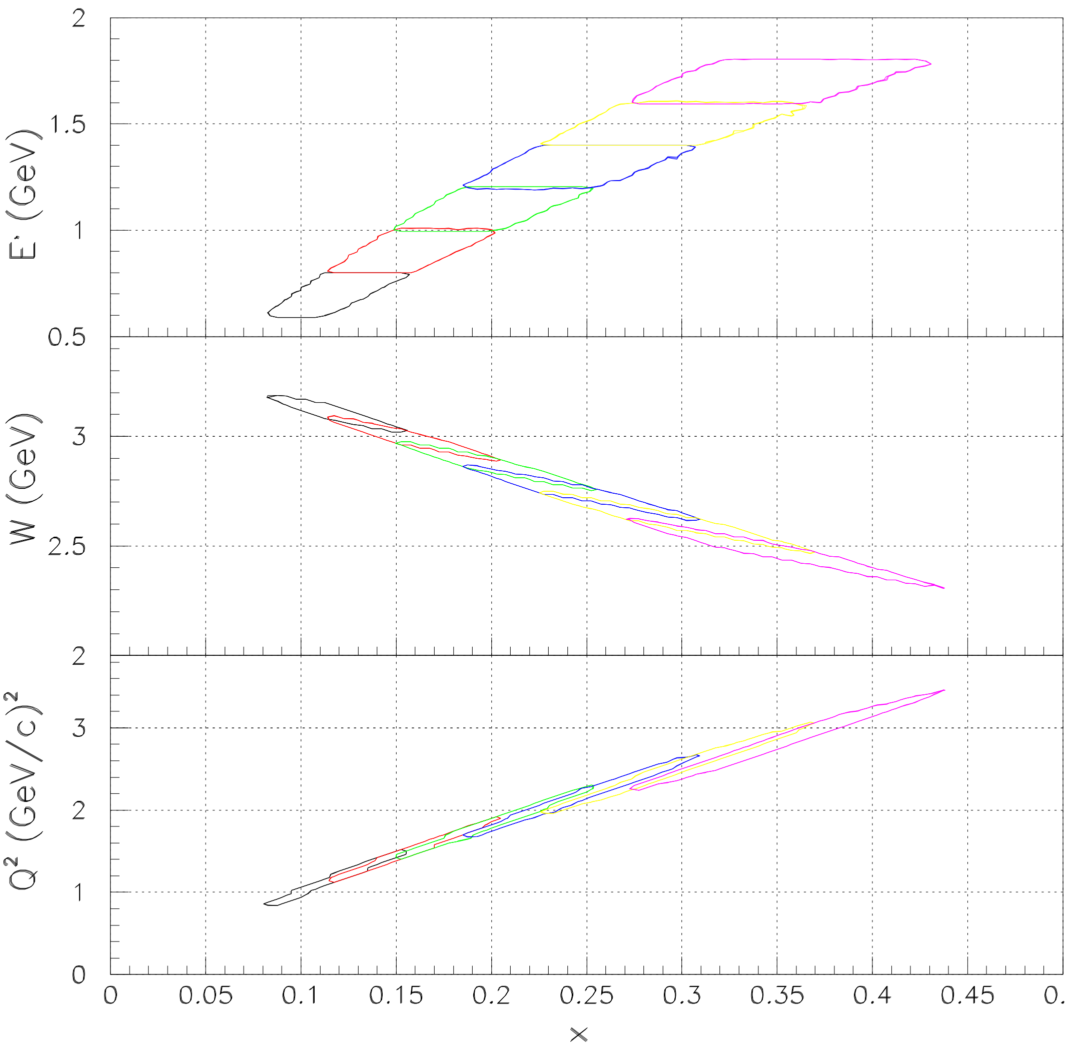

Figure 7: The phase space coverage in (x, W) plane and in (x, Q^2) plane corresponding to six bins in E' labeled by different colors.

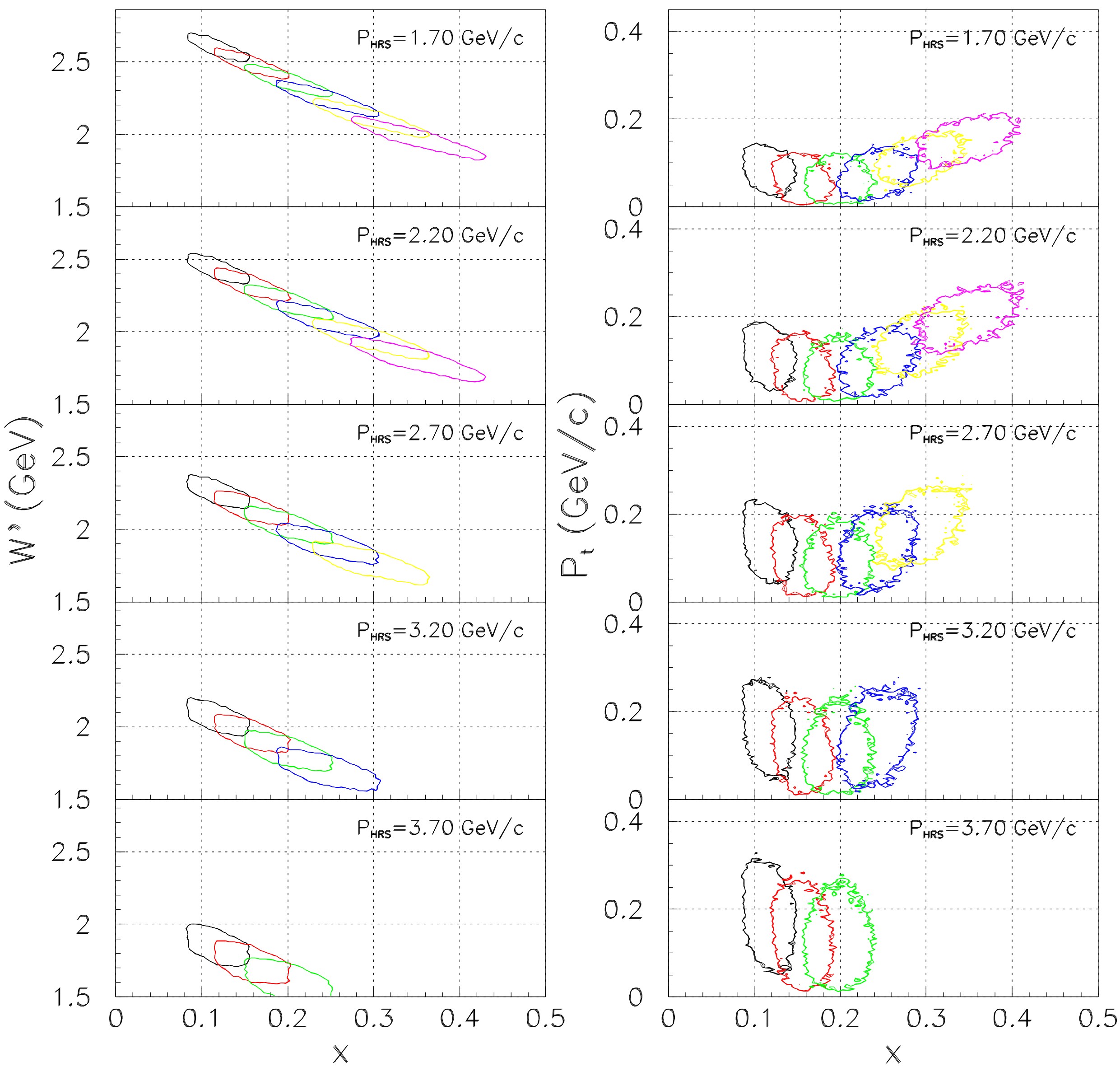

Figure 8: The phase spaces for four different HRS settings in (x, W') and (x, p_t) plane. Several bins of E' are plotted following the same color code as in the previous plots. The phase space for the kinematics with hadron momentum of 3.7 GeV/c is also shown, though they are not in the kinematic table.

2.3 Experimental Setup

The Hall-A floor configuration for this experiment has been checked with the Hall A mechanical design group to make sure there is no interference between different elements. The BigBite magnet will be located 2.4 meters away from the target at an angle of 30°. Well-collimated shielding is planned in front of the magnet to reduce background. Shielding between the detector package and the beam dump will also be required.

The standard 15 cm Hall A cryogenic Hydrogen and Deuterium targets will be used. Target density will be monitored by pressure and temperature measurements. Single arm electron events will also be used to correct for target density changes.

Left Side HRS Spectrometer and Detectors

The left side HRS spectrometer will have the recently commissioned RICH detector in addition to its standard configuration. A threshold gas Cherenkov together with lead-glass shower counters will give excellent e/π^- separation. The RICH detector, in combination with an aerogel Cherenkov counter, will provide clean separation of $\pi^+/K^+/p$ or π^-/K^- in a wide kinematic range. The performance of the RICH detector has been demonstrated in the recently completed Hall A hypernuclear experiment (E94-107) [20] (see Fig. 9).For the hypernuclear experiment, for momentum up to 2.5 GeV, the pion rejection of 10^{-3} was achieved for pion and kaon separation. Since the momentum range for this proposal will be up to 3.7 GeV, a new radiator with a lower index of refraction will be needed.

The Electron Arm Spectrometer and Detectors

We plan to put the BigBite spectrometer at 2.4 meters drift from the target as the electron arm. The platform will need to be re-designed to accommodate the new location. The detector package configuration will be the same as in the G_E^n(E02-013) [21] experiment. The following considerations were taken into account:

- To provide particle ID and good pion rejection, well-segmented shower detectors should be used. A pre-shower and a shower calorimeter will be needed, as in the planned G_E^n experiment.
- Reconstruction of the vertex in the target gives a large reduction factor on accidental events. Reasonable target reconstruction can be done with BigBite which has simple optics.
- Knowledge of the electron energy from the calorimeter allows the trajectory of electrons to be reconstructed even with multiple hit events in the chambers.

The detector configuration of the BigBite spectrometer is shown in Fig 10. A GEANT Monte Carlo simulation [21] was performed to guide the design of the electron arm detector package. The expected momentum resolution in E02-013 with different drift chamber position resolutions is shown in Fig. 11. Since this experiment does not seek to resolve any structures in the final states, the requirement for momentum and angular resolution is very modest. The space between the scattering chamber and the detector package will be air (no special helium bag is required). The momentum resolution designed for E02-013 will be more than adequate for this proposal. The angular resolution will be about 3.0 mrad in each direction, causing only a few MeV spread in P_t reconstruction. The vertex resolution will be better than 2.0 cm (along the beam).

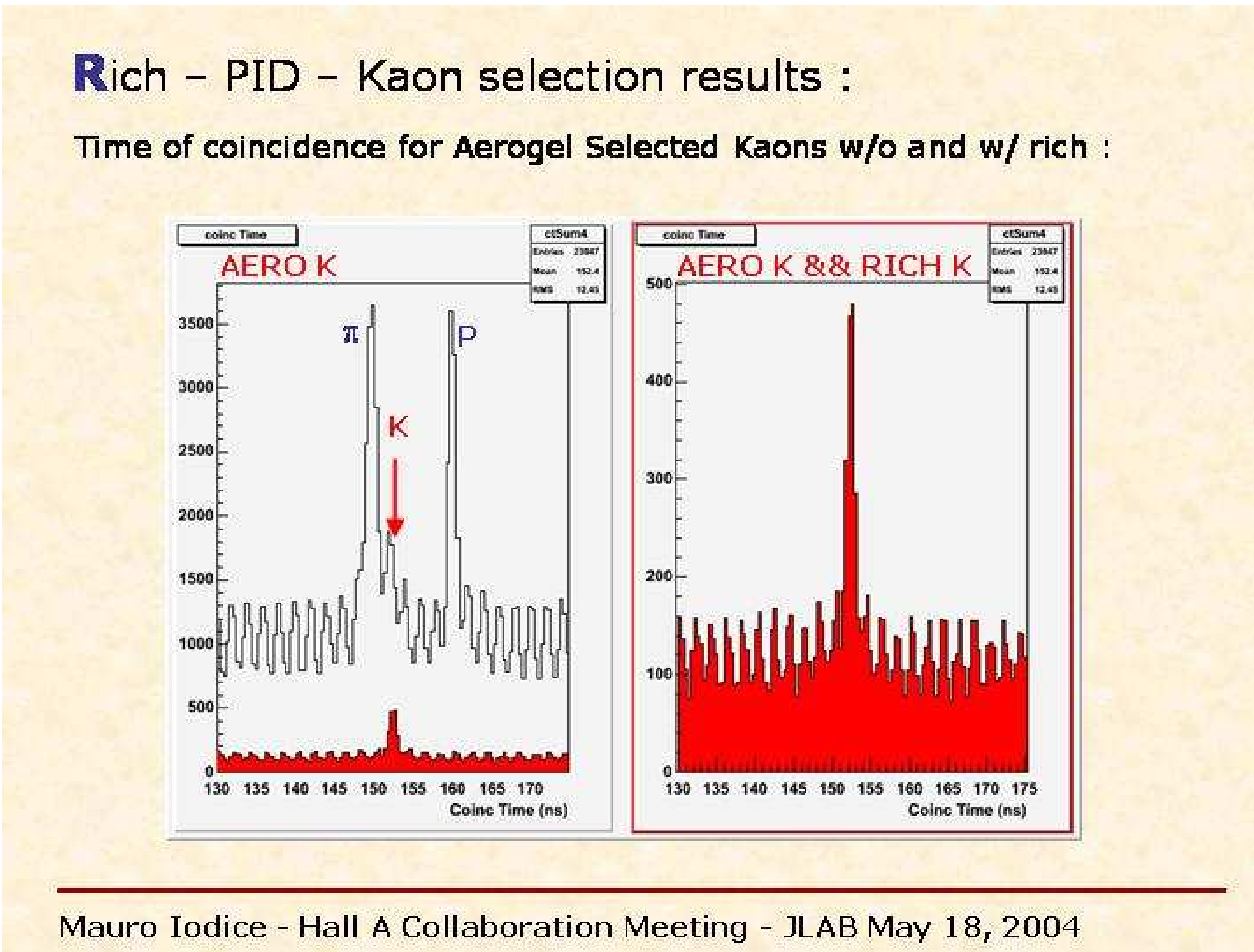

Figure 9: The Hall A RICH detector performance during hypernuclear experiment.

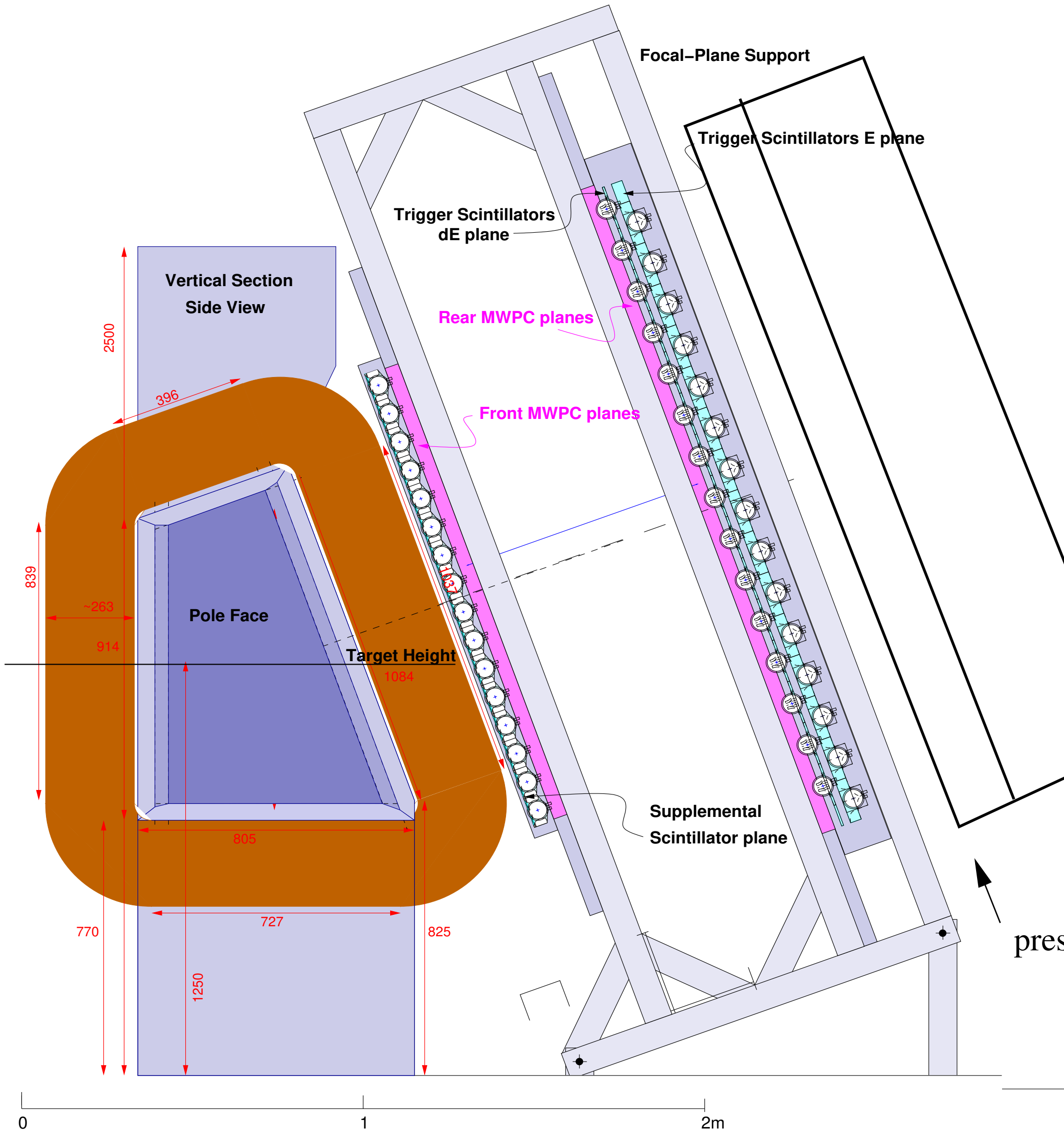

Figure 10: The side view of the BigBite spectrometer with its detector package. The location of two wire chambers and two lead glass arrays are shown.

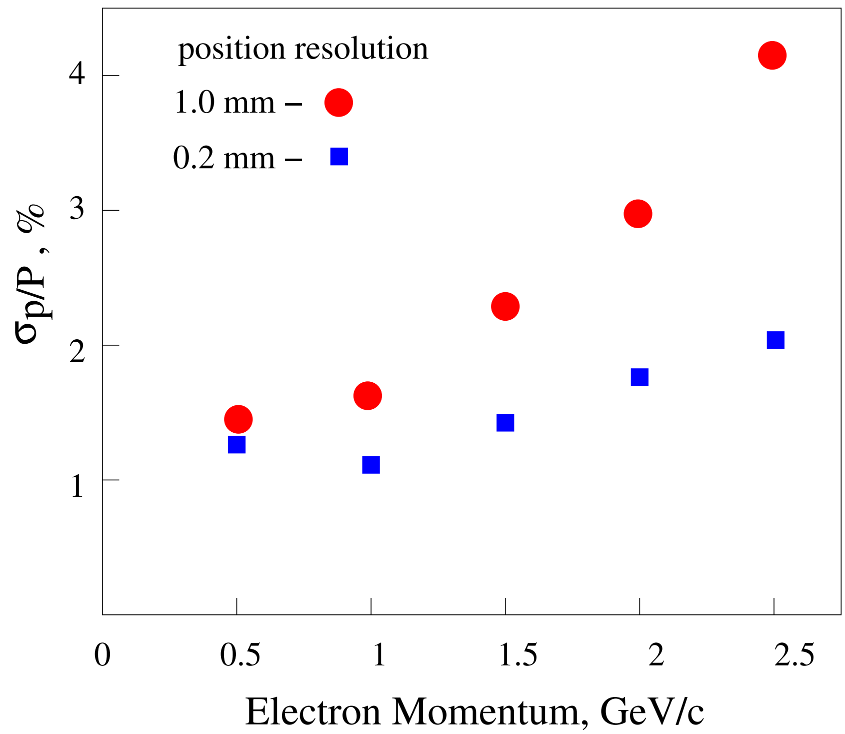

Figure 11: The momentum resolution of the BigBite spectrometer.

Fig. 12 shows Monte Carlo simulation results[22] of the BigBite momentum acceptance and the expected solid angle as a function of interaction point.

2.4 Background rates and accidental coincidence rates.

Single electron rates in each arm are estimated using deep inelastic scattering cross sections. Due to its largely open geometry and relatively weak dipole field, the BigBite spectrometer will accept electrons with momenta starting roughly from 0.2 GeV up to the beam energy. In Table 2 the singles electron rates in each 200 MeV bin in BigBite are listed. We assume a 5 μA beam on a 15 cm liquid hydrogen target. The single arm π^-/e^- ratio [24] should not be more than 15:1 based on data collected in a similar kinematics during experiment E99-117. Therefore, total negative charged particle rates in BigBite should be less than 80 kHz. With the planned pre-shower and shower detector(almost the same as the right arm HRS pre-shower and shower package in size and configuration) a pion rejection factor of 100 can be easily achieved.

Positive pion, positron, and proton rates were estimated by P. Degtiarenko's Monte Carlo simulation code GDINR [23]. The integrated rates for particles with momentum above 0.1 GeV are: positrons less than 1.0 kHz, π^+ less than 70 kHz, and protons less than 10 kHz. Therefore, the overall charged particle rate in BigBite above 0.1 GeV momentum should be less than 160 kHz for the hydrogen target. Singles rates for the deuterium target should be comparable under similar luminosity. We realize that the low energy background on the BigBite wire chambers will likely be the instrumentation limitation for this experiment. Compared with the background situation in E02-013, this experiment has a factor of four

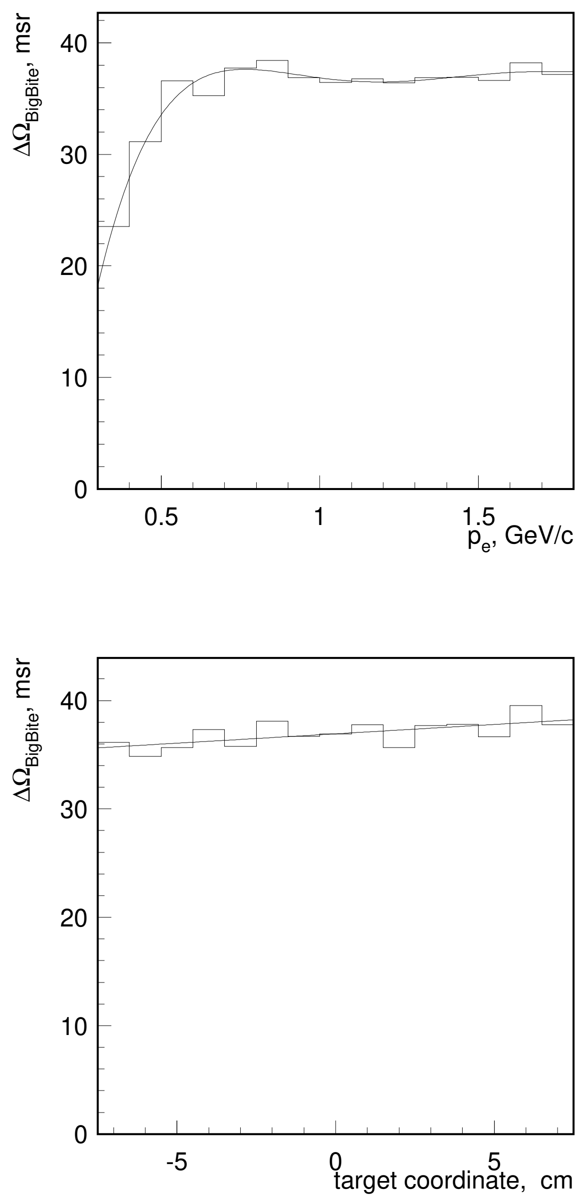

Figure 12: The BigBite solid angle acceptance with a drift distance of 1.5 m as a function of the particle momentum (top) and the interaction point along the beam (bottom). For the proposed experiment, the solid angle will be around 16.7 msr with the drift distance of 2.4 m.

Table 2: Rates of single electrons from DIS for each 200 MeV bin of the BigBite spectrometer, with a 5 μA beam and a 15 cm liquid Hydrogen target. Single electron rates on a Deuterium target are comparable with a 2.5 μA beam.

E'	θ_e	$\langle x \rangle$	W	Q^2	$\text{Rate}_{(e,e')}$
GeV	deg.		GeV	GeV^2	Hz
0.300	30.0	0.05	3.33	0.48	860.4
0.500	30.0	0.08	3.22	0.80	796.2
0.700	30.0	0.11	3.11	1.13	655.8
0.900	30.0	0.15	3.00	1.45	545.7
1.100	30.0	0.19	2.88	1.77	460.7
1.300	30.0	0.24	2.76	2.09	389.5
1.500	30.0	0.29	2.63	2.41	324.0
1.700	30.0	0.34	2.49	2.73	261.5
1.900	30.0	0.40	2.35	3.05	201.2
2.100	30.0	0.46	2.20	3.38	144.6
2.300	30.0	0.53	2.03	3.70	94.3
2.500	30.0	0.61	1.85	4.02	53.2
2.700	30.0	0.70	1.65	4.34	23.5
2.900	30.0	0.80	1.43	4.66	6.5
Total Electron Singles Rate in BigBite					**$\sim$ 5 kHz**

less solid angle and a factor of 6 more luminosity in terms of the number of nucleons in the beam. By taking BigBite to a large drift distance, we will have an extra 1.2 meter of space before the magnet to build up heavy shielding and install a thick collimator. We will also put shielding between the BigBite and the beam dump. Furthermore, we plan to shield the edge area of the wire chambers to reduce chamber activities caused by low energy particles.

A background rate test of the BigBite spectrometer is planned in Hall A. Improvements on the design of the detector and shielding are very much expected. In addition, several other experiments are planning to use BigBite before this experiment starts. Knowledge of the origin of the background will help us further reduce the low energy particle rates. Since this experiment has relatively high coincidence rates, further reduction of the BigBite solid angle is also an option.

For the left HRS at 6°, the electron singles rate in the worst case is less than 100 kHz, and positron rates are less than 1 kHz. Pion singles rates are less than 100 kHz, and proton singles rates are of the order of a few kHz. The combination of the threshold gas Cherenkov and two layers of lead-glass shower counters should provide sufficient e^-/π^- and e^+/π^+ separation. The RICH detector and aerogel Cherenkov in combination with tracking corrected time-of-flight information will provide good separation for π^+, K^+ and proton, or π^- and K^-.

Based on the singles rate from the recent Hall A Pentaquark experiment E04-012 [25] which used the septum magnet in a similar setting as in this proposal, we estimated that the total charged pion single's rate in the left-HRS should be less than 60 kHz. With a BigBite electron singles rate around 5 kHz, we expect the accidental (e, π) rate to be less than 30 Hz within the 100 ns coincidence time window. The Hall A time-of-flight resolution is better than 1.0 ns, therefore a 2.0 ns timing cut will reduce the accidental rate to less than 0.6 Hz. Since both arms have an vertex resolution of better than 2.0 cm, an additional accidental reduction factor of 7.5 can be achieved. Therefore, the final accidental coincidence rates should be less than 0.08 Hz, a factor of 6 less than the real's rate for the worst case of this experiment.

3 Count Rate Estimate and Beam Time Request

3.1 Coincident $(e, e'\pi)$ Cross Section Model and Rate Estimate.

The model of coincident cross sections has the following inputs:

- The inclusive (e, e′) cross sections for protons and deuteron.
- A parameterization of the fragmentation functions $D^+(z)$ and $D^-(z)$ as a function of Q^2.
- A model of the transverse momentum distributions of pions as fragmentation products.

The inclusive deep inelastic (e, e') cross section can be expressed in the quark parton model as:

$$\frac{d^2\sigma}{d\Omega dE'} = \frac{\alpha^2(1+(1-y)^2)}{sxy^2}\frac{E'}{m_N\nu}\sum_i e_i^2\left(q_i(x,Q^2)+\bar{q}_i(x,Q^2)\right) \tag{30}$$

where m_N is the nucleon mass, $y = \nu/E$, $s = 2Em_N + m_N^2$. The quark distribution functions $q_i(x, Q^2)$ and $\bar{q}_i(x, Q^2)$ are taken from the CTEQ6M global fits [26]. The predicted inclusive cross sections agree with SLAC data [27] to better than 20% within the kinematic region of this proposal.

The semi-inclusive $(e, e'h)$ cross section relates to the quark fragmentation function $\mathrm{D}_i^h(z, Q^2)$ and the total inclusive cross section σ_{tot} through:

$$\frac{1}{\sigma_{tot}} \frac{d\sigma(e, e'h)}{dz} = \frac{\sum_i e_i^2 f_i(x, Q^2) D_i^h(z, Q^2)}{\sum_i e_i^2 f_i(x, Q^2)}. \quad (31)$$

The two light quark fragmentation functions, $D^+(z, Q^2)$ and $D^-(z, Q^2)$, relate to each other approximately through [28]:

$$D'(z) = \frac{D^-(z, Q^2)}{D^+(z, Q^2)} = \frac{1-z}{1+z}. \quad (32)$$

HERMES data [29] show some deviation from the above approximation, which can be parameterized [30] as $D'(z) = (1-z)^{0.008358}/(1+z)^{1.984}$. The fragmentation functions, such as $D^\pi(z, Q^2)$=$(D^+(z, Q^2) + D^-(z, Q^2))/2$, were from BKK parameterization [31] based the world e^+e^- annihilation data. The recent HERMES results [32] show that the pion transverse momentum ($p_\perp$) distribution follows the form of $e^{-bp_\perp^2}$ with $b = 4.661 \pm 0.019\mathrm{GeV}^{-2}$ for π^+ production and $b = 4.694 \pm 0.024\mathrm{GeV}^{-2}$ for π^- production. We used the above HERMES results and realistic spectrometer acceptances to estimate the count rates. In this proposal, we placed the HRS close to the $\vec{q}$ direction to have relative large azimuthal coverage.

With a 5 μA/2.5 μA beam on a 15 cm standard Hall-A cryogenic hydrogen/deuterium target, the luminosity is 2.0×10^{37} (nucleon) $\mathrm{cm}^{-2}\mathrm{s}^{-1}$. We lower the current for deuterium kinematics to maintain the same luminosity and keep the BigBite spectrometer in a similar environment as the hydrogen kinematics. The HRS spectrometer with the septum magnet has an angular acceptance of $\Delta\theta_{hor} =^{+24}_{-19}$ mrad and$\Delta\theta_{ver} = \pm 50$ mrad, and a momentum acceptance of $\pm 4.5\%$ [33]. The BigBite spectrometer will be kept in one setting throughout this experiment. It will detect charged particles over a momentum range of $0.6 \sim 1.8$ GeV/c with reasonable resolution. Because of this large momentum bite, data can be binned in six x-bins from $x = 0.11$ to $x = 0.34$. An electron detection efficiency of 90% is assumed.

To study the violation of factorization, we take four different P_π settings between 1.7 and 3.2 GeV/c. The beam times are chosen such that a sample of 12k,24k,24k,12k coincident events could be collected for P_π=1.7,2.2,2.7,3.2 GeV/c respectively at $x = 0.19$, for both π^- and π^+ production and for both hydrogen and deuterium target. The data with $W' > 1.8$ GeV will be combined together for each x so that statistical accuracy on r_1 (r_2) will be better than 0.015 (0.03) in all x bin. The estimated count rates and beam time allocations for each x-bin are listed in Table 3.

The beam time request is summarized in Table 4. In addition to 490 hours of production beam time, we request 20 hours for dummy target yield check, 30 hours for BigBite detector check and optics calibration and 10 hours for HRS magnet polarity change, 10 hours for HRS momentum changes, 10 hours for target movements and 10 hours for HRS short single arm runs. Since the planned BigBite spectrometer and its detector package will be used in similar ways in several other Hall A experiments, some shared calibration beam time is expected to be available before this experiment starts. Additional Hall A facility development time will also be available to the BigBite collaboration for additional calibrations and detector shakedown.

4 Systematic Uncertainties and Expected Results

Since we plan to measure yield ratios rather than the absolute cross sections, sensitivity to instrumental effects are minimized. The recently completed Hall A super-Rosenbluth exper-

Table 3: Estimated coincident rates (in Hz) in each 0.2 GeV E'-bin for four HRS momentum settings (P_{HRS} in GeV/c) on a Hydrogen target; the average x values for each bin are listed. Beam times (in hours) under each HRS setting are listed in the right two columns. The rates are based on a 5 μA beam on a 15 cm liquid Hydrogen target. Count rates for those bins with an average $W' < 1.6$ GeV are not listed.

P_{HRS}	π^+	π^-	π^+	π^-	π^+	π^-	π^+	π^-	π^+	π^-	π^+	π^-	T^{π^+}	T^{π^-}
	$x = 0.11$		0.15		0.19		0.24		0.29		0.34		Hours	
1.70	0.23	0.17	0.21	0.14	0.18	0.12	0.15	0.10	0.12	0.07	0.09	0.05	23	35
2.20	0.39	0.26	0.34	0.21	0.28	0.17	0.23	0.13	0.17	0.09	0.12	0.06	30	49
2.70	0.54	0.34	0.45	0.27	0.36	0.20	0.28	0.14	0.19	0.09	0.12	0.06	23	42
3.20	0.65	0.38	0.52	0.28	0.40	0.20	0.28	0.13	0.18	0.08	-	-	11	21
Time on Hydrogen Target													**234**	
(Time on Deuterium Target)													(256)	
Total Data Collection Time													**490**	

Table 4: Summary of beam time request.

Item	Time (Hours)
Data Production Beam Time	490
BigBite Optics and Calibration	30
Dummy Target Yield	20
Target Movements	10
HRS Magnet Polarity Change	10
HRS Momentum Changes	10
HRS Single Arm Runs	10
Total Beam Time Requested	**580 (24 days)**

iment [34] has demonstrated that many relative systematic uncertainties could be controlled at a few tenth of percent level. The major concern of systematic uncertainties comes from the difference between π^+ and π^- detection efficiencies and in luminosity corrections. Since we planned enough overlap on different pion momentum settings, local detection efficiency differences could be monitored and corrected. We will use the recently installed LUMI detector [35] to continuously monitor luminosity. Beam charge and target density measurement as well as spectrometer single events rates can provide additional luminosity monitoring. The relative luminosity measurement will reach a precision of better than the 0.5% level.

The radiative correction differences between $(e, e'\pi^+)$ and $(e, e'\pi^-)$ reaction could introduce systematic uncertainties in extracting quark and anti-quark distribution ratios. This kind of higher order radiative correction difference is expected to be relatively small in the yield ratios. The difference will mainly depend on the difference of the cross sections for π^+ and π^-, which is smaller than 0.5% in the z range of this proposal. A procedure of radiative corrections in $(e, e'\pi^\pm)$ reaction is under development at JLab.

Another issue in the interpretation of this experiment is the effects of final state interaction in the $H(e, e'\pi)$ and $D(e, e'\pi)$ reactions. We intentionally chose the pion momentum to be higher than 1.7 GeV/c to minimize the effect of final state interaction. We also chose to avoid the resonance region by taking W' as high as possible ($1.8 < W' < 2.6$ GeV) and observing the pions directly along the momentum transfer. Thus we expect the effects of final state interaction can be calculated with high precision.

Table 5 summarizes the statistical and systematic uncertainties for the physics quantities. The experimental systematic uncertainties are decomposed into the target (d/p) dependent part and the meson charge (m^-/m^+) dependent part while the absolute normalization part cancels in the ratio. The target dependent systematic uncerntainties including luminosity and other target related effects is assigned to be 0.7%. We may use one x bin point, for example $x = 0.11$, to get a normalization factor for the deuterium yields by comparing to the world Drell-Yan data. It helps that the BigBite spectrometer collect data for different x bins simultaneously and r_H is not very sensitive to the π^+ yield. The meson charge dependent systematic uncertainties are dominated by the PID corrections (0.5%) and the radiative corrections (0.5%). It is worth mentioning that the r_H measurement is not sensitive to the meson charged related uncertainties at all. The ratio of the fragmentation functions (D^-/D^+) is needed for the r_H measurement and will be measured in this experiment. The uncertainty on D^-/D^+ includes 0.011 of statistical uncertainty and 0.006 of experimental systematic uncertainty based on the data at $x = 0.34$. The parton distribution function will be used to extract $\bar{d} - \bar{u}$ and $\bar{d}/\bar{u}$ from r_H measurement. The results are not very sensitive to the parton distributions. We assumed 5% uncertainty in the world parameterization of $u - d$ and 10% in that of $\bar{u} + \bar{d}$. The uncertainties for kaons are larger than those for the pions and the estimations are also listed in the table.

We will have enough data to determine the onset of the generalized factorization with high precision (better than 0.015 on r_1, 0.03 on r_2, 0.02 on r_H). Fig.13 shows the projected r_1 and r_2 as functions of z. We should see in our kinematic conditions the z-independent behavior as in the HERMES experiment and in E00-108. The yield ratios will directly be the quark distribution ratios as $r_1 = (d+\bar{d})/(u+\bar{u})$ and $r_2 = (d-\bar{d})/(u-\bar{u})$. Strong constraints can be made to the quark distribution functions over the measurement region.

On the other hand, our measurement could demonstrate a transition to the factorization regime, where some kinematics will show the evidence of the factorization while others will start to show deviation from the factorization. A clear demonstration of such a transition

Table 5: Experimental uncertainties at $x = 0.19$ and $z = 0.55$.

Quantity	Value	Statistical	d/p	m^-/m^+	D^-/D^+
$r_1 = (d+\bar{d})/(u+\bar{u})$	0.628	0.010	0.018	0.001	-
$r_2 = (d-\bar{d})/(u-\bar{u})$	0.474	0.016	0.007	0.005	-
$r_H = (\bar{d}-\bar{u})/(u-d)$	0.113	0.013	0.019	0.001	0.015
$t_2^K = (d-\bar{d})/(u-\bar{u})$	0.474	0.057	0.015	0.004	-
D_d^K/D_u^K	0.93	0.17	0.15	0.01	-

will be very interesting.

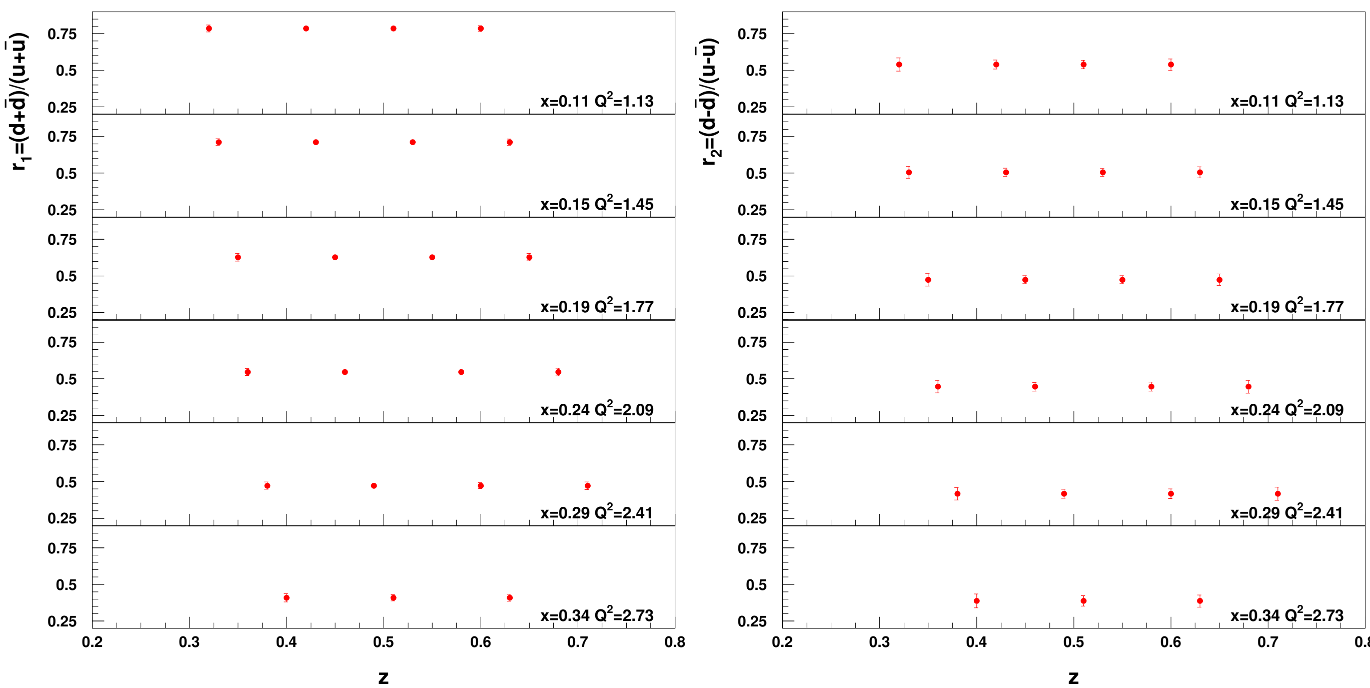

Figure 13: Projected z dependence of r_1 and r_2 with statistical uncertainties.

4.1 Expected results on light quark and anti-quark distribution ratios.

The projection on r_1 and r_2 measurements are shown in Fig. 14. The error bars on the data points are statistical only.

The projection of $\bar{d}/\bar{u}$ are shown in Fig. 15 together with Fermilab E866 data points. Also shown are the projected results in $(\bar{d}-\bar{u})/(u-d)$ and $\bar{d}-\bar{u}$ together with the world data.

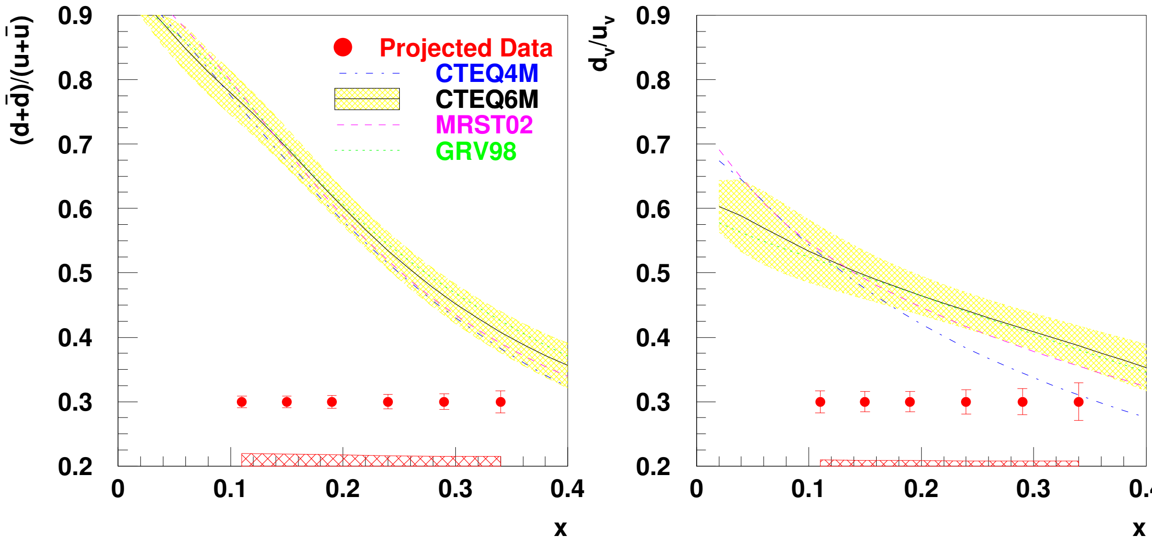

Figure 14: The projected data on r_1 and r_2 with statistical uncertainties. Systematic uncertainties are shown as bands on the bottom of the plots.

4.2 Kaon production results.

With the excellent kaon detection capability, the $(e, e'K^+)$ and $(e, e'K^-)$ events will be collected in the data at the same time. The expected number of kaon events is approximately a factor of 10 lower than for the pions. Table 5 shows the expected statistical accuracy for the kaon $t_2^K(x)$ measurement. This would allow a very significant independent test of the factorization, as well as providing an independent measurement of d_V/u_V.

Fig.16 shows the expected precision of the measurement of the ratio $D_d^{K^\pm}/D_u^{K^\pm}$. The three curves [19,36,31,37] are parameterizations of the fragmentation functions which fit to the e^+e^- data. One of the fits (Kretzer2000) has the constraint of equal light sea fragmentations, $D_{\bar{d}}^{K^+} = D_{\bar{u}}^{K^+}$. The other two fits do not have this constraint. The expected precision is sufficient to distinguish between the Kretzer2000 and the other two curves, therefore should be able to test whether there is indeed a large $\bar{d}/\bar{u}$ flavor asymmetry in the kaon fragmentation functions.

5 Relation to other experiments

We note that Hall-C experiment E00-108 [1] was proposed to test "Duality in Meson Electroproduction" using the $(e, e'\pi)$ reaction. The experiment took data last year. Preliminary results are available now. The data [2] demonstrated that the data are consistent with generalized factorization for the optimized JLab kinematics.

With luminosity of $(1-5) \times 10^{32}$ cm^{-2}s^{-1} for unpolarized beam at HERMES, six orders of magnitude lower than this proposal, it will be very time consuming to collect data to the same statistical accuracy as we proposed here. In addition, for a large detector setup as in HERMES, detection efficiency control at different part of the detectors to a precision of 0.5% would prove to be very challenging.

Fermilab P906 is a proposed extension of Fermilab fixed target E866 experiment using a high intensity 120 GeV proton beam out of the Fermilab Main Injector. The P906 proposal

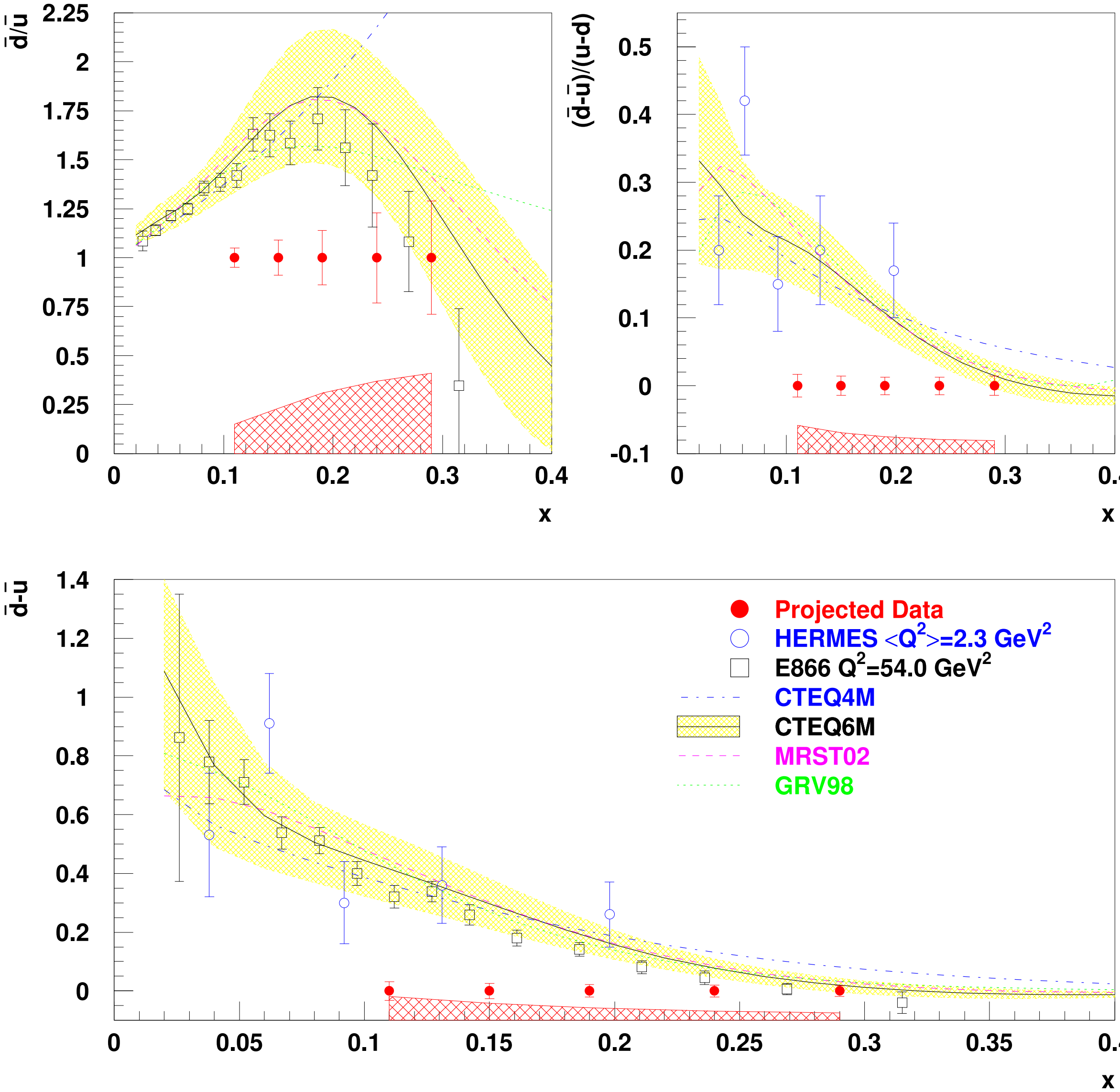

Figure 15: The projected data, with statistical uncertainties, on $\bar{d}/\bar{u}$,$(\bar{d}-\bar{u})/(u-d)$ and $\bar{d}-\bar{u}$ together with the world data and fits. Systematic uncertainties were shown as bands on the bottom of the plots.

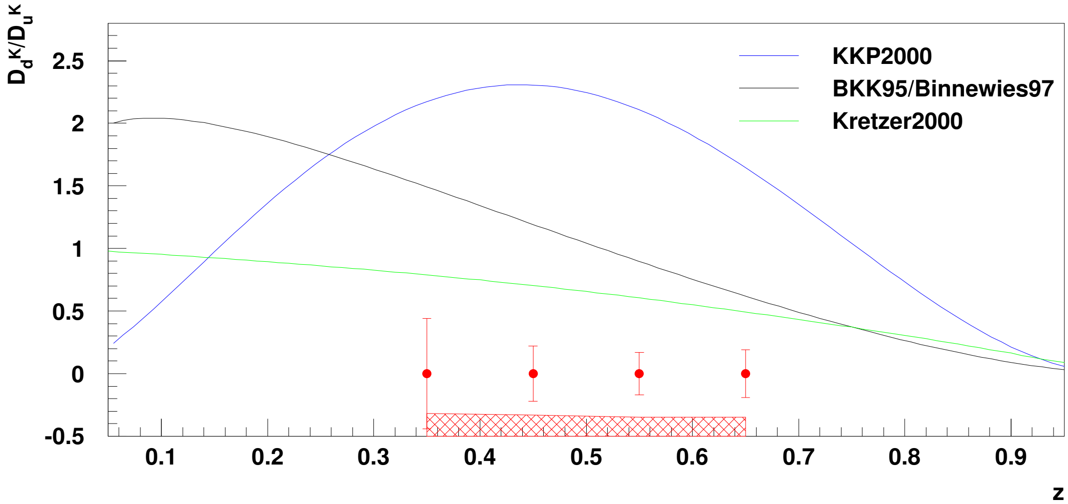

Figure 16: The projected data, with statistical uncertainties, on $D_d^{K^\pm}/D_u^{K^\pm}$. Three curves are different fits to the e^+e^- data. Kretzer2000 has the constraint of equal light sea fragmentations, $D_{\bar{d}}^{K^+} = D_{\bar{u}}^{K^+}$. The other two fits do not have this constraint. Systematic uncertainties were shown as bands on the bottom of the plots.

would increase the x coverage to 0.45 with much improved statistics over E866 data. Using the completely different Drell-Yan ratio technique, P906 is not in competition with this proposal.

Very small forward angle access is almost impossible in Hall C and Hall B. This fact makes the high precision deep-inelastic semi-inclusive reactions, such as in this proposal, inaccessible to these two Halls at 6 GeV energy without extensive hardware development efforts.

The proposed study of the flavor dependent fragmentation functions and factorization, will greatly help the other experiments using SIDIS to study nucleon spin-flavor decomposition [38] and transversity [39] and the future SIDIS program with JLab 12 GeV [40] energy upgrade.

6 Summary

In conclusion, we propose to make a high precision measurement of deep inelastic semi-inclusive π^+/π^- and K^+/K^- yield ratios on hydrogen and deuterium. We will extract light quark and anti-quark distribution ratios and study the flavor dependence of the fragmentation functions. The data will also provide tests of the generalized factorization. JLab at 6 GeV will allow us to reach W high enough to be in the deep inelastic scattering region. At a higher x range and much better statistical precision than the HERMES experiment, we will be able to independently test the Fermilab E866 results with a completely different reaction mechanism. If proven successful, this method would allow us to extend the measurement to quark spin density distributions and to strange-sea quark distributions. A total of 24 days of beam time is requested for our experiment with 6 GeV unpolarized beam in Hall A.

References

1. R. Ent, H. Mkrtchyan and G. Niculescu, JLab E00-108 " Duality in Meson Electroproduction"
2. R. Ent and H. Mkrtchyan, private communications.
3. K. Ackerstaff *et al.*, *Phys. Rev. Lett.* **81**, 5519 (1998); *Phys. Lett.* B **464**, 123 (1999); A. Airapetian *et al.*, *Phys. Rev. Lett.* **92**, 012005 (2004).
4. A. Airapetian *et al.*, *Phys. Lett.* B **562**, 182 (2003).
5. X. Ji, J. P. Ma and F. Yuan, hep-ph/0404183 (2004).
6. K. Gottfried, *Phys. Rev. Lett.* **18**, 1174 (1967).
7. P. Amaudruz, *et al.*, *Phys. Rev. Lett.* **66**, 2712 (1991).
8. F. M. Steffens and A. W. Thomas, *Phys. Rev.* C **55**, 900 (1997), S. Kumano, Phys. Rep. Vol. 303, 4(1998) pp183-257.
9. S. D. Ellis and W. J. Stirling, *Phys. Lett.* B **256**, 258 (1991).
10. J. Levelt *et al.*, *Phys. Lett.* B **263**, 498 (1991).
11. E. A. Hawker, *et al.*, *Phys. Rev. Lett.* **80**, 3715 (1998); R. S. Towell *et al.*, *Phys. Rev.* D **64**, 052002 (2001)
12. H. L. Lai, *et al.*, Eur. Phys. J, C12, 375 (2000).
13. A. D. Martin, R. G. Roberts, W. J. Stirling, and R. S. Thorne, Eur. Phys. J, C4, 463 (1998).
14. S. Kumano, Phys. Rep. 303, 183 (1998).
15. G. T. Garvey and J. C. Peng, Prog. Part. Nucl. Phys. 47,203 (2001).
16. M. Glück, *et al.*, *Z. Phys.* C **67**, 433 (1995).
17. W. Melnitchouk, *et al.*, *Phys. Lett.* B **435**, 420 (1998).
18. M. Alberg et al., Phys. Lett. B389, 367 (1996).
19. B.A. Kniehl, G. Kramer, B. Potter, *Nucl. Phys.* B **582**, 514 (2000) or eprint:hep-ph/0010289.
20. S. Frullani, F. Garibaldi, J. LeRose and P. Markowitz, JLab E94-107; M. Iodice, presentation at the Hall A Collaboration Meeting (2004).
21. G. Cates, K. McCormick, B. Reitz and B. Wojtsekhowski, JLab E02-013: "Measurement of the Neutron Electric Form Factor G_E^n at High Q^2" (2002).
22. V. Nelyubin, BigBite Monte Carlo simulation, private communications.
23. P. Degtiarenko, private communications.
24. J. W. Lightbody, Jr. and J. S. O'Connell, Computers in Physics, 1988
25. P. Reimer and B. Wojtsekhowski, JLab E04-012.
26. J. Pumplin, *et al.*, JHEP 07, 012,(2002) or eprint:hep-ph/0201195.
27. L. W. Whitlow, SLAC-Report-357, March (1990).
28. R. D. Field and R. P. Feynman, *Nucl. Phys.* B **136**, 1 (1978).
29. P. Geiger, Ph.D. Thesis (1998).
30. D. Gaskell, private communication.
31. J. Binnewies, B. A. Kniehl and G. Kramer, *Phys. Rev.* D **52**, 4947 (1995).
32. B. Hommez, Ph.D. Thesis (2003)..
33. J. LeRose, private communication, and Hall-A Hypernuclear Collaboration, Technical Notes on Septum Magnets Design, September (1996).
34. J. Arrington, R. Segel, JLab E01-001; R. Segal, presentation as a JLab seminar.
35. R. Suleiman, 'A Concetptual Design of Hall A Lumi Monitor', (2003).
36. S. Kretzer, *Phys. Rev.* D **D62**, 054001 (2000) or eprint:hep-ph/0003177.

37. Binnewies, eprint:hep-ph/9707269.
38. D. Day, X. Jiang, M. Jones, JLab PR03-104.
39. J. P. Chen, X. Jiang, J. C. Peng, JLab E03-004.
40. pCDR for the 12 GeV Upgrade Science and Equipment.